Journal of The Electrochemical Society, **155** (5) F110-F115 (2008)
0013-4651/2008/155(5)/F110/6/$23.00 © The Electrochemical Society

Correlation Between the Distribution of Oxide Functional Groups and Electrocatalytic Activity of Glassy Carbon Surface

Nelio R. Vettorazzi,[a] Leonides Sereno,[a,*] Masaaki Katoh,[b] Michiya Ota,[b] and Luis Otero[a,*,z]

[a]*Departamento de Química, Universidad Nacional de Río Cuarto, X5804BYA Río Cuarto, Argentina*
[b]*Department of Chemistry, Gunma College of Technology, Gunma 371-8530, Japan*

Oxidative electrochemical pretreatment on glassy carbon (GC) electrodes in aqueous media produces changes in the relative densities of oxidized species present on the material surface. These changes vary with both applied potential and time procedure. The GC surface oxidation treatment not only increases the oxygen-containing group coverage but also causes lattice damage, producing a highly porous dielectric film. In this work we report the gradual relationship between the kinetics of the heterogeneous charge transfer after different pretreatment procedures and the surface distribution of oxidized species in GC measured through electron spectroscopy for chemical analysis. The lack of faradaic current observed when the electrode surface is oxidized under the constant-potential regime is proposed to be due to changes in the lattice structure, observed by scanning electron microscopy. This fact is important in systems where carbon materials are used as electrodes under the continuous-oxidation regime, such as high-performance liquid chromatography electrochemical detectors, batteries, capacitors, and for the generation of polymers by potentiostatic oxidation.
 [DOI: 10.1149/1.2895065]

Manuscript submitted October 25, 2007; revised manuscript received February 11, 2008. Available electronically March 28, 2008.

The characteristic of carbon materials for electrochemical uses has been widely described in the bibliography.[1-4] In the last years attention has been focused on the surface structural modification, mainly on the control of pore size and distribution and the increase in active area. Some examples are the studies on glassy carbon (GC) and reticulated GC (RVC, an open-macropore foam material with high void volume and surface area) for capacitor electrodes,[5,6] storage batteries, and the manufacture of semiconductors.[7] RVC also has multiple applications in environmental analysis,[8,9] extractive metallurgical industry,[10] and fuel cells. This rigid structure allows infused materials to be held in controlled pore sizes. Another structural modification with specific target applications in micro-, meso-, and macroscale are the formation of multiwalled carbon nanotubes,[11-14] polyaniline-coated single-walled carbon nanotube composite electrodes,[15] new functional materials obtained by derivatization of carbon surfaces,[16-18] nanopillar arrays of GC by anodic Al_2O_3 nanoporous (meso) templates,[19] etc.

Other uses of GC, pretreated GC, or modified-composite GC materials, (that do not necessarily involve an increase in surface area) are for electroanalysis and electrocatalysis.[20-29] But, an important problem in GC application is the electrochemical-response reproducibility related to the electrode pretreatment.[30,31]

Diverse investigations showed that the electrodes obtained by different voltammetric methods had different behaviors to the adsorption of organic molecules.[32-34] It has also been reported[30] that the possible difference in void volumes (or etch pits) obtained by different voltammetric methods might affect the electrochemical response.

More specifically, in the cases where potentiodynamic or potentiostatic electrochemical pretreatment were used, it has been reported[5] that oxidative activation in acid aqueous media without a reduction step conduces to the formation of a nonconductor film, where redox couples are unable to produce charge transfers.[35] This situation is easily reverted by the application of less-anodic potentials or reduction steps. Thus, it is important to make a distinction between these pretreatments, even when the procedure is restricted only to the oxidation of GC surface in acidic media, as the obtained results are strongly conditioned by the potential program used. Recently, Yamazaki et al. reported a simple electrochemical method for determining the number of carboxyl groups on GC electrodes. The authors concluded that strong electrochemical oxidation of GC increases not only the total number of carboxyl groups but also the surface area of the GC.[36] Liu et al. analyzed the heterogeneous electron-transfer properties on organic-monolayer modified GC and concluded that the electrode material has an important influence on the electron-transfer rate.[37] As in this last case, the electrochemical response of solution-based redox probes is commonly used to detect and monitor the formation and stability of films grafted into GC and other electrode surfaces.[38]

In this work, we report the gradual relationship between electrochemical activity of modified GC material and its surface state. The superficial oxidized group distribution [analyzed by electron spectroscopy for chemical analysis (ESCA)] changes with the pretreatment procedure have a direct correlation with the electrochemical response of the electrode. Moreover, the observation of a nonconductive soft material produced by the constant-oxidation regime allows the interpretation of the loss of electrochemical activity of the electrode when it is under continuous oxidation. This would be important when GC electrode is used under potentiostatic conditions in processes like high-performance liquid chromatography (HPLC) electrochemical detectors, batteries, capacitors, electrosynthesis, or base electrode for the deposition of electroactive polymer, because the process could occur at the potentials where the oxidation of GC takes place at the same time.

Experimental

Instrumental, electrode material, and chemicals.— GC material was generously provided by the Mitsubishi Pencil Company of Japan (pyrolisis temperature 1400°C) in the form of 0.1 mm thick plates. Electric contact was achieved by a gold wire. Ultrapure water was obtained from Labconco equipment.

Voltammetric measurements were performed with an Autolab PG30 potentiostat–galvanostat. The ohmic drop was carefully compensated for by the positive feedback technique. All the experiments were conducted under N_2 atmosphere and temperature control (25 ± 0.1°C), maintained with a Lauda K 4 R thermostat–cryostat. All the potentials are referenced to a saturated calomel electrode. The auxiliary electrode was a Pt foil with a large area. The cell was a PAR Polarographic Top Assembly.

The growth of electrogenerated surface oxides was performed by oxidation in 1 M H_2SO_4 (Merck, purified agent). 5 mM Fe^{2+} in 1 M H_2SO_4 used as a model couple was prepared from $FeSO_4 \cdot 7H_2O$ (Sigma ACS).

Electrochemical pretreatment procedures.— Unless another condition is reported, potentiodynamic GC surface modification was performed by a different number of oxidative cycles in 1 M H_2SO_4 between −0.5 and 2.1 V at 0.15 V s^{-1}. Also, the effect of the poten-

* Electrochemical Society Active Member.
z E-mail: lotero@exa.unrc.edu.ar

tial at which the scan is reversed for the modification (E_λ) was analyzed while keeping constant the number of modification cycles.

Before using the electrode in electron-transfer rate determination, each electrode was stabilized in 1 M H_2SO_4 by cycling in the non-oxidative potential range (from −0.5 to 1.0 V at 0.15 V s^{-1}) in order to achieve background current reproducibility.

Modification of the GC electrode surface was also done by the potentiostatic method in 1 M H_2SO_4 at 2.1 V using different times, obtaining a distinct degree of oxidation (measured through the anodic charge involved). In order to avoid surface reduction, the circuit was opened after each oxidation period. This technique is different from those where the final potential after the oxidative pretreatment is allowed to reach an active surface for heterogeneous charge transfer.[5,35] The observed heterogeneous charge-transfer constant (k^0_{obs}) for the kinetic analysis of the redox couple Fe^{2+}/Fe^{3+} (used as a model for catalytic inner-sphere charge transfer at the GC surface[39]) was determined from voltammetric data using the simulation program DigiSim 2.1 (Bioanalytical Systems, West Lafayette, IN). A common procedure for all simulations to fit the experimental data was followed: (*i*) blank subtraction: for GC electrodes with different degrees of modification, the baseline was subtracted for each voltammogram before simulation; (*ii*) the charge-transfer coefficient α was assumed to be 0.5; (*iii*) E^0 and diffusion coefficients of Fe^{2+}, Fe^{3+} were taken from Ref. 29; (*iv*) model parameters: exponential grid factor $B = 0.05$, potential step=0.001 V; and (*v*) k^0_{obs} was allowed to vary until a good fit was obtained.

ESCA and scanning electron microscopy measurements.— ESCA was performed on a Shimadzu ESCA 3400. The spectra were recorded with a pass energy of 20 eV. The base pressure of the system was typically 1×10^{-6} Torr. The electron emission angle was 90°. The samples were investigated as received for industrial GC, while the electrochemically modified electrodes were removed from the electrolyte, rinsed several times with water, immersed in an ultrasonic bath with ultrapure water, dried by a nitrogen stream, and introduced into the ESCA vacuum chamber.

Scanning electron microscopy (SEM) samples were investigated with a JEOL JSM-5600 scanning electron microscope in order to determine the microstructure of the films generated. The films were visible in SEM in terms of contrast and structural differences.

Results and Discussion

Figure 1 shows a GC voltammogramm after 30 oxidation–reduction cycles between −0.5 and 2.1 V in H_2SO_4 1 M, where a first layer of surface oxygen-containing groups is fully generated.[35,40] According to the interpretation given in Ref. 41 the peaks developed in zone I correspond to the redox processes associated with the presence of the mentioned groups, while in zone II the oxidation of H_2O_2 formed by oxygen reduction in zone IV is verified. Finally, in zone III water is discharged with oxygen evolution. The inset shows a cyclic voltammogram in zone I, where the redox processes involving the oxidation and reduction of the electroactive surface oxygen-containing groups that contribute to the electrode pseudo-capacitance are evidenced. The anodic charge involved in this process is a useful parameter for the characterization of the surface state of the electrode. The Q_0 parameter, defined from the Osteryoung equation,[42] is obtained by measuring the anodic charge (Q_a) between −0.5 and 0.8 V at several scan rates. As has already been described,[35-41] Q_a varies linearly with the reciprocal of the square root of the sweep potential rate ($v^{-1/2}$) in the range 0.020–0.60 V s^{-1}. The Q_a value extrapolated to $v \to \infty$ gives Q_0. This parameter is proportional to the number of exposed or superficial sites susceptible to oxidation. In the absence of adsorption, Q_0 can be regarded as the double-layer and pseudo-capacitance charges.

Figure 2 displays voltammograms of Fe^{2+} oxidation, all normalized by peak current. As can be shown, the couple Fe^{2+}/Fe^{3+} becomes more reversible as the number of modification cycles increases. The kinetics of this couple directly depends on the grade of oxidation of the carbon surface state, as has been established previously.[39] The observed heterogeneous charge-transfer constant (k^0_{obs}) values increase with Q_0 (Fig. 3), which is electrochemical proof that the kinetic performance of the Fe^{2+}/Fe^{3+} couple is affected by the presence of oxidized surface groups. The observed electrocatalysis can be assigned to the reactive sites associated with the pseudo-capacitance charge of the electrode.

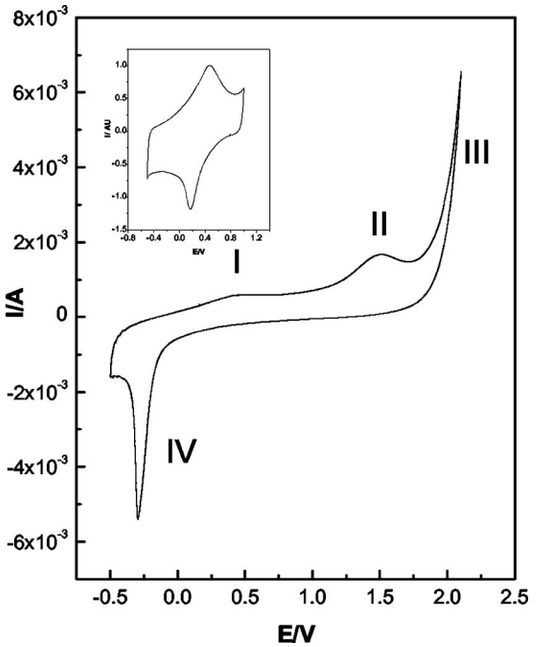

Figure 1. Cyclic voltammogram of GC in 1 M H_2SO_4 after 30 cycles of potentiodynamic activation. (Inset) Zone I between −0.5 and 1.0 V. v = 0.15 V s^{-1}.

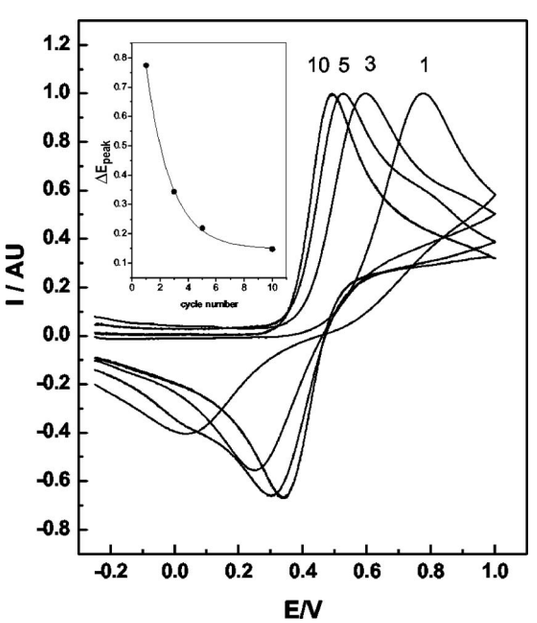

Figure 2. Cyclic voltammograms of Fe^{2+}/Fe^{3+} 5 mM (as $FeSO_4$) in 1 M H_2SO_4 after a variable number of cycles (indicated in the figure) of potentiodynamic activation. (Inset) ΔE_{peak} vs number of cycles. v = 0.04 V s^{-1}.

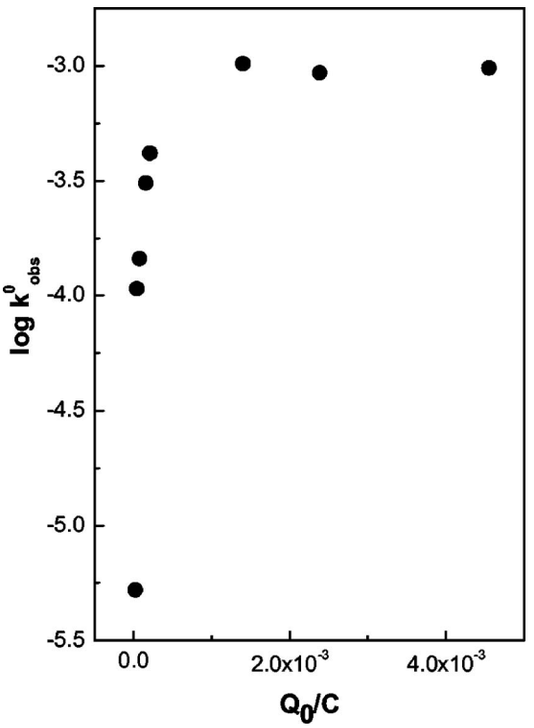

Figure 3. Log k^0_{obs} for Fe^{2+}/Fe^{3+} couple as a function of Q_0 parameter.

Figure 4 shows ESCA spectra of GC samples. For industrial GC, a typical C 1s peak at 284.78 eV was detected. The electro-oxidized samples yield three oxygen functions of our interest responsible for primary C 1s chemical shifts. The peak at 287 eV was attributed to the C–OH, the peak at 288.5 eV to the C = O, and the peak at

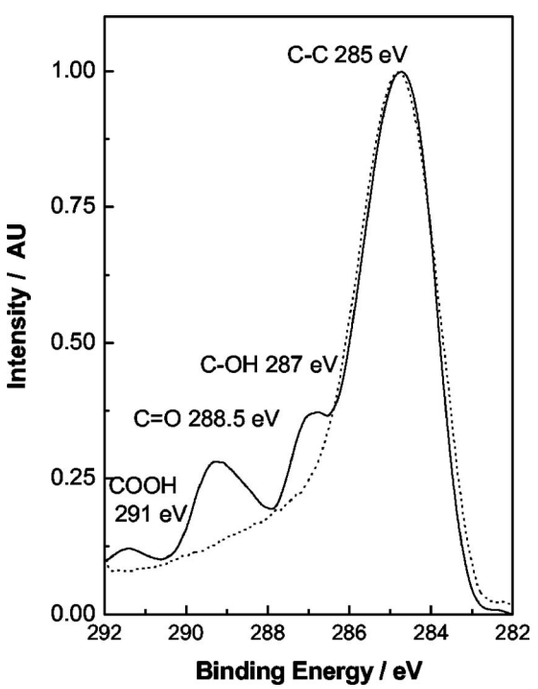

Figure 4. ESCA from industrial (dotted line) and modified (continuous line) GC electrodes.

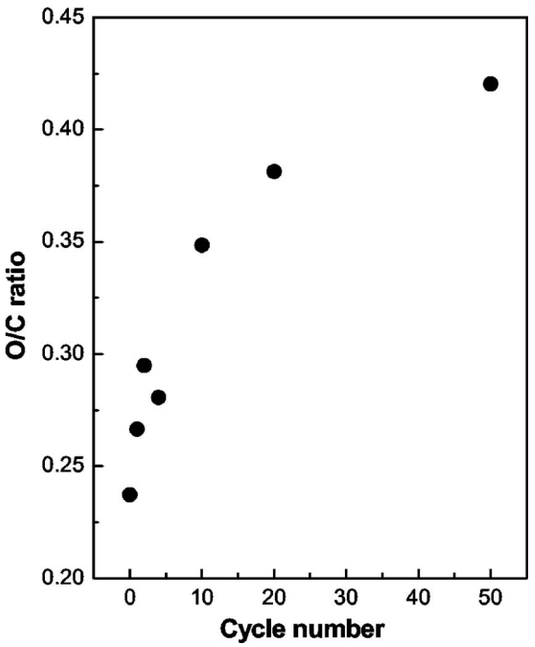

Figure 5. O/C ratio vs cycle number of potentiodynamic activation.

291 eV to the COOH surface group. The formation of functional surface groups is reflected in the amount of oxygen that can be detected in the ESCA spectra. The relative oxygen content was determined by integration of the O 1s emission peak (533.7 eV). The relationship between the O/C ratio and the number of modification cycles (Fig. 5) shows that the gradual increment in the modification procedure correlates with an increment in the surface oxidized groups. In conclusion, the cycle number in the modification procedure can control the number of these surface groups. In this way, we can control the gradual modification of the GC surface in order to analyze it by ESCA and make a correlation with the electrocatalytic activity of the carbon surface. As the kinetic performance of the Fe^{2+}/Fe^{3+} couple is affected by the presence of oxidized groups, we analyzed the electrocatalytic capacity of the GC electrode as a function of the O/C ratio determined by ESCA analysis, Fig. 6. k^0_{obs} increases with the amount of oxygen surface groups and reaches a plateau when the surface has an O/C ratio of about 0.35, or 12–13% C = O (Fig. 6, inset). This fact shows a threshold of oxidation degree, beyond which the kinetic performance of the GC surface cannot be improved. As has been recently reported,[36] strong oxidation does not greatly increase the number of carboxyl groups per surface area.

When the number of modification cycles is kept constant (5 cycles) while changing the potential at which the scan is reversed for the modification procedure (E_λ), a relevant effect over the electrocatalytic capacity (k^0_{obs}) of GC electrode is observed. Figure 7 shows the changes in the fashion of the Fe^{2+} oxidation voltammograms, with the corresponding increment in the k^0_{obs}, which is depicted in Fig. 8. Additionally, ESCA analysis allows the observation that while the amount of C–O surface functionalities remains nearly constant, those corresponding to the presence of C = O-containing groups increase as E_λ in the modification procedure becomes more anodic[36] (Fig. 9). This is evidence that not only is the presence of oxygen-containing groups responsible for the electrochemical activity of the CG electrode, but the identity is also important. Our results agree with those given in Ref. 43, where k^0_{obs} for the Fe^{2+}/Fe^{3+} couple increases with the surface C = O density, measured through the 1140 cm^{-1} Raman peak area, corresponding to the formation of an adduct between dinitrophenylhydrazine and the carbonyl surface

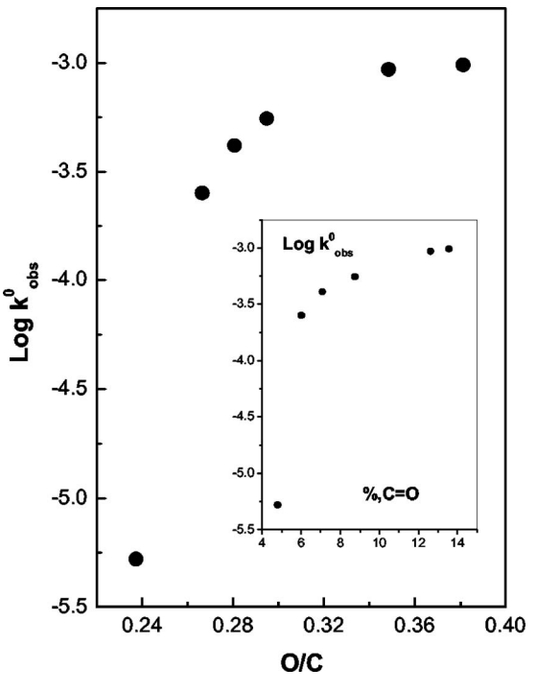

Figure 6. Log k^0_{obs} for Fe^{2+}/Fe^{3+} couple as a function of O/C relationship. (Inset) k^0_{obs} for Fe^{2+}/Fe^{3+} couple as a function of % C = O.

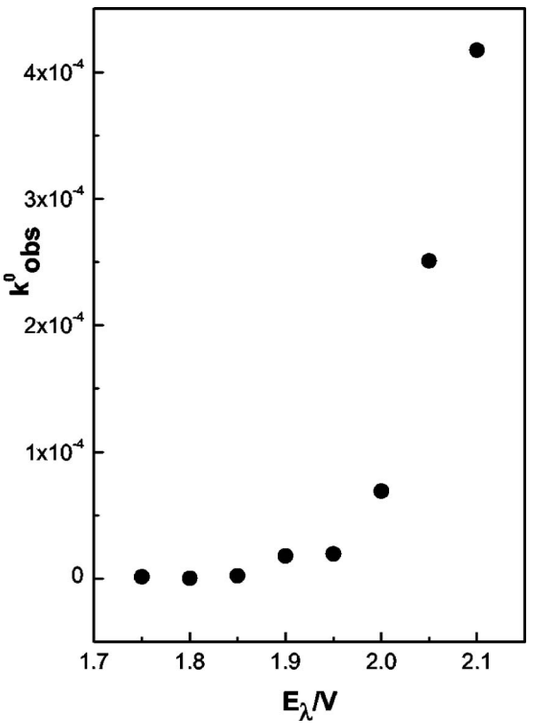

Figure 8. k^0_{obs} for Fe^{2+}/Fe^{3+} couple as a function of reverse potential. Potentiodynamic activation at constant number of cycles (five).

groups in a GC electrode. Figure 10 shows the relationship between C = O percent in GC surface and k^0_{obs} for Fe^{2+} oxidation. It can be seen in Fig. 8 and 10 that at $E_\lambda > 1.95$ V, k^0_{obs} quickly increases, in agreement with the increment of the pseudo-first-order kinetics with respect to carbonyl surface density (Fig. 9).

Potentiostatic oxidation pretreatment methods used with GC electrodes develop different effects over the kinetics of heterogeneous charge transfer than those that involve a reduction step. For example, it has been stated[44] that the anodization of GC electrodes without reduction was found to be detrimental for Mo(VI) discharge. In our case, when the electrode is oxidized at 2.1 V in 1 M H_2SO_4 media for 5 min and the circuit is opened to avoid reduction currents, the Fe^{2+} discharge is not observed, and gradual reactivation of the charge transfer is obtained only after reduction pulses. However, the distribution of oxygen-containing surface functionalities obtained from ESCA analysis before the reduction step are similar to those obtained after the cyclic modification procedure. Then, the difference observed could be attributed to electronic and structural aspects, which affect the electron-transfer kinetics. Ellipsometric measurements[40] showed that the optical properties of electrogenerated oxides (EGO) are different after oxidation and reduction steps. The ellipsometric n and k values indicated an almost-dielectric layer after oxidation and an absorbing layer after reduction. Although the uses of these optical results are not straightforward as a measure of the conductivity, the increases of absorption, faradaic currents, and capacity suggest that the reduction of the layer increase its conductivity and electrochemical activity.[45]

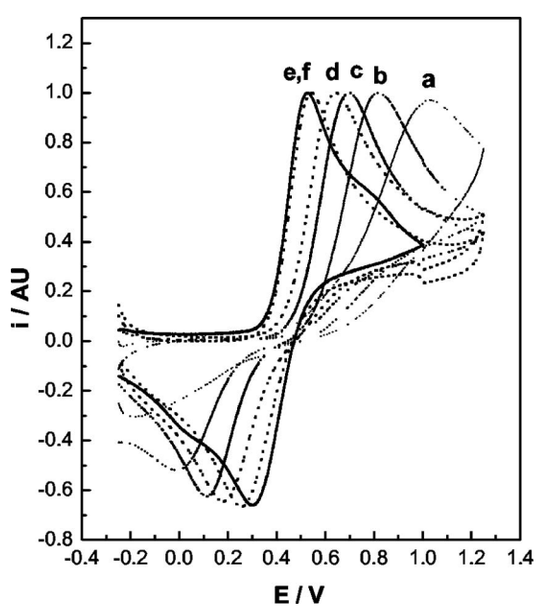

Figure 7. Cyclic voltammograms of Fe^{2+}/Fe^{3+} 5 mM (as $FeSO_4$) in 1 M H_2SO_4 after variable reverse potential (E_λ) for potentiodynamic modification, constant cycle number (five), $v = 0.04$ V s^{-1}: (a) 1.80, (b) 1.85, (c) 1.90, (d) 1.95, (e) 2.00 and (f) 2.05 V.

As we pointed out,[35] the lack of faradaic response with redox couples of both outer- or inner-sphere charge transfer is observed when GC electrodes are oxidized and no reduction process is allowed. This fact seems to indicate the presence of a dielectric over the GC surface, in agreement with the model reported in Ref. 5.

We also analyzed the GC by SEM before and after cyclic electrochemical modification (Fig. 11a-d) in order to determine the microstructure of the films generated. The films were visible in SEM in terms of structural differences between bulk and electrogenerated film. At a low modification degree (Fig. 11b) the occurrence of damage centers is clearly observed on the GC surface. These initiator centers are the cores where star-fashioned channels are developed when the oxidation degree of the GC surface increases (Fig. 11c). The origin of these structural effects on the GC surface by the electro-oxidation procedure is not clear, but it could be related to the geometry of the graphite nets in the carbon structure. At higher modification degrees an increase in surface roughness was observed,

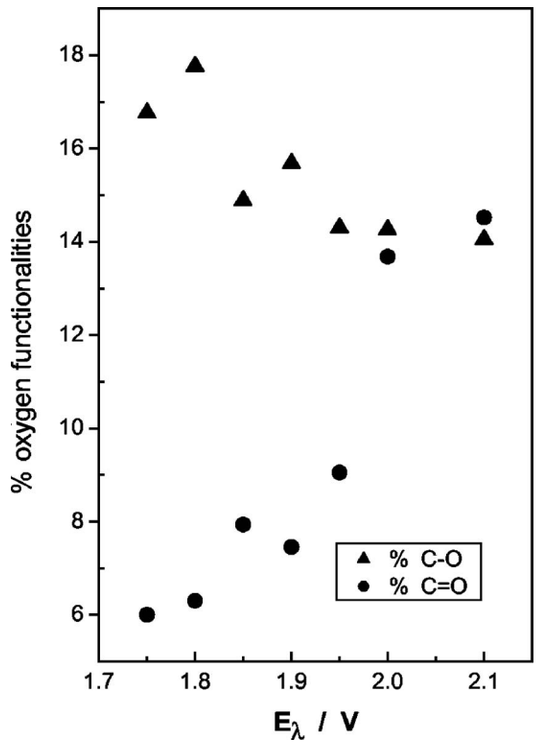

Figure 9. Distribution of surface functionalities (C = O, C–O) as a function of reverse potential.

with marked damage in the graphite nets. These layers are porous, having a high internal surface area that could result in high volumetric capacitance (Fig. 11d). The films obtained by potentiostaic oxidation, without a reduction step, show a different contrast in the SEM image (Fig. 12). The structural changes observed after surface

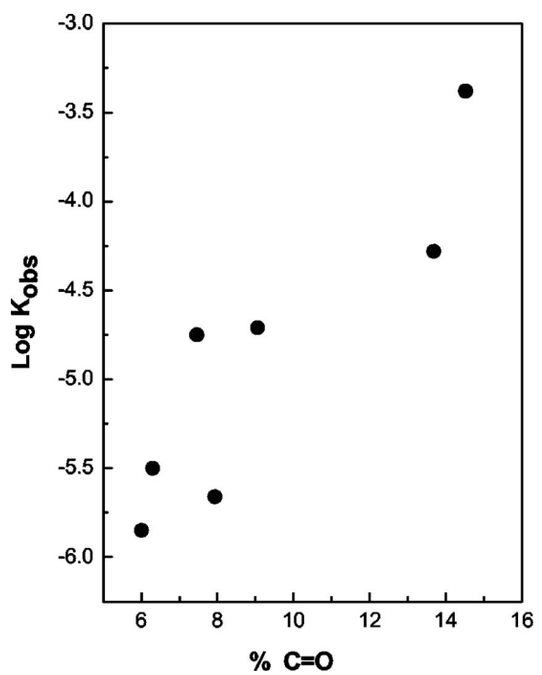

Figure 10. Correlation between k^0_{obs} and % C = O surface occupation.

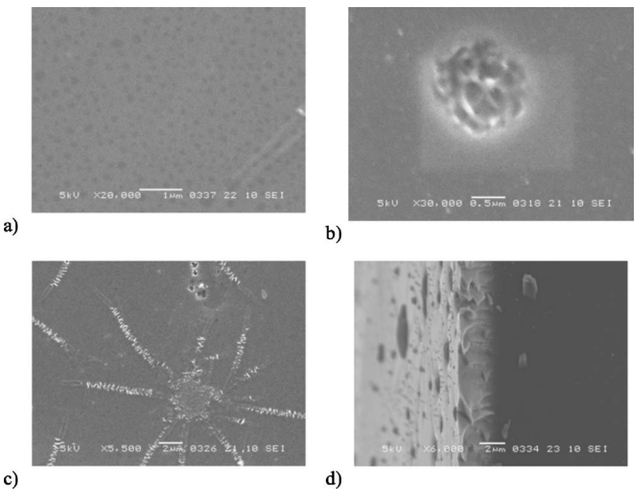

Figure 11. (a) Industrial (unmodified) GC surface, (b) after potentiodynamic modification (two cycles, E_λ = 2.1 V, υ = 0,15 V/s), (c) idem 5 cycles, and (d) edge image after 40 cycles.

oxidation could be related to the electrochemical performance of GC electrodes. According to our electrochemical analyses, potentiostatic oxidation leads to an electrochemically inactive dielectric layer. In Fig. 12 (a view of the electrode edge), a soft material is observed that could be responsible for the insulating properties of the generated surface. This material produces an SEM image different than those obtained with a GC surface that has been oxidized and reduced by repetitive cycles (Fig. 11d). However, it is not clear if the low electronic conductivity is due to a low density of electronic states (and a corresponding low density of charge carriers, as in highly ordered pyrolytic graphite[46]) or to the presence of a disordered layer[47] in the GC surface, where the graphite nets are far away from each other, creating a nonconductive material.

Conclusions

The gradual modification of the GC surface was analyzed by ESCA and correlated with the electrocatalytic activity of the carbon material. This work shows that the kinetics of the Fe^{2+}/Fe^{3+} couple correlates with the carbonyl reactive sites, and analysis allowed the identification of a threshold potential for the generation of catalytic centers for the probe couple. SEM images taken at different degrees of modification showed the occurrence of initiator centers on the GC surface as cores where damaged channels develop. The EGO films are porous and, in potentiostatic conditions of GC modification

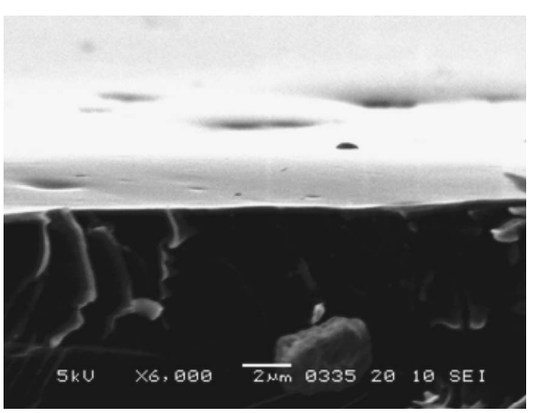

Figure 12. Edge image of GC surface after potentiostatic modification (300 s, E = 2.1 V).

without a reduction step, a non electroactive material is produced. The low electronic conductivity responsible for the total lack of faradaic response to either inner- or outer-sphere charge-transfer reactions is due to structural effects, because the reactive site distributions obtained from ESCA analysis are similar to those obtained after the cyclic modification procedure. This fact is important in systems where carbon materials are used as electrodes under continuous oxidation, such as HPLC electrochemical detectors, batteries, capacitors, and for the generation of polymers by potentiostatic oxidation.

Acknowledgments

We are grateful to Consejo Nacional de Investigaciones Científicas y Técnicas (CONICET, Argentina), Agencia Nacional de Promoción Científica y Tecnológica (ANPCYT, Argentina), and the Secretaría de Ciencia y Técnica de la Universidad Nacional de Río Cuarto (SECYT-UNRC) for financial support. The Research Cooperation Division of the Japan Society for the Promotion of Science (JSPS) supported the visit of L.O. under the Bilateral Exchange Program (JSPS-CONICET) agreement.

Universidad Nacional de Río Cuarto assisted in meeting the publication costs of this article.

References

1. G. M. Jenkins and K. Kawamura, in *Polymeric Carbons, Carbon Fibre, Glass and Char*, Cambridge University Press, Cambridge, England (1976).
2. K. Kinoshita, in *Carbon, Electrochemical and Physico-chemical Properties*, John Wiley & Sons, New York (1988).
3. Z. W. Zhang, D. A. Tryk, and E. B. Yeager, in *Electrochemistry of Carbon*, S. Sarangapani, J. R. Akridge, and B. Schumm, Editors, PV 84-5, p. 158, The Electrochemical Society Proceedings Series, Pennington, NJ (1984).
4. R. L. McCreery, in *Electroanalytical Chemistry*, Vol. 17, A. J. Bard, Editor, Marcel Dekker, New York (1991).
5. M. G. Sullivan, B. Schnyder, M. Bärtsch, D. Alliata, C. Barbero, R. Imhof, and R. Kötz, *J. Electrochem. Soc.*, **147**, 2636 (2000).
6. T. A. Centeno, M. Hahn, J. A. Fernandez, R. Kotz, and F. Stoeckli, *Electrochem. Commun.*, **9**, 1242 (2007).
7. J. M. Friedrich, C. Ponce-de-Leon, G. W. Reade, and F. C. Walsh, *J. Electroanal. Chem.*, **561**, 203 (2004).
8. N. Peña, A. J. Reviejo, and J. M. Pingarrón, *Talanta*, **55**, 179 (2001).
9. A. Alvarez-Gallegos and D. Pletcher, *Electrochim. Acta*, **44**, 853 (1998).
10. V. Reyes-Cruz, I. González, and M. T. Oropeza, *Electrochim. Acta*, **49**, 4417 (2004).
11. T. Wang, M. Wang, X. Hu, X. Qu, F. Zhao, and S. Dong, *Langmuir*, **21**, 12068 (2005).
12. Q.-L. Chen, K.-H. Xue, W. Shen, F.-F. Tao, S.-Y. Yin, and W. Xu, *Electrochim. Acta*, **49**, 4157 (2004).
13. K. Wu, S. Hu, J. Fei, and W. Bai, *Anal. Chim. Acta*, **489**, 215 (2003).
14. A. Salimi, H. Mam-Khezri, R. Hallaj, and S. Zandi, *Electrochim. Acta*, **52**, 6097 (2007).
15. Y.-K. Zhou, B.-L. He, W. Zhou, J. Huang, X.-H. Li, B. Wu, and H.-L. Li, *Electrochim. Acta*, **49**, 257 (2004).
16. S. S. C. Yu and A. J. Downard, *Langmuir*, **23**, 4662 (2007).
17. K. H. Vase, A. H. Holm, K. Norrman, S. U. Pedersen, and K. Daasbjerg, *Langmuir*, **23**, 3786 (2007).
18. S. E. Creager, B. Liu, H. Mei, and D. DesMarteau, *Langmuir*, **22**, 10747 (2006).
19. S. Rahman and H. Yang, *Nano Lett.*, **3**, 439 (2003).
20. A. Parra, E. Casero, L. Vazquez, J. Jin, F. Pariente, and E. Lorenzo, *Langmuir*, **22**, 5443 (2006).
21. X. Feng, C. Mao, G. Yang, W. Hou, and J.-J. Zhu, *Langmuir*, **22**, 4384 (2006).
22. F. J. López-Garzón, M. Domingo-García, M. Pérez-Mendoza, P. M. Alvarez, and V. Gómez-Serrano, *Langmuir*, **19**, 2838 (2003).
23. S. Uchiyama, H. Watanabe, H. Yamazaki, A. Kanazawa, H. Hamana, and Y. Okabe, *J. Electrochem. Soc.*, **154**, F31 (2007).
24. M. Kullapere, G. Jürmann, T. T. Tenno, J. J. Paprotny, F. Mirkhalaf, and K. Tammeveski, *J. Electroanal. Chem.*, **599**, 183 (2007).
25. X. Lin, G. Kang, and L. Lu, *Bioelectrochemistry*, **70**, 235 (2007).
26. M. L. S. Silva, M. B. Q. Garcia, J. L. F. C. Lima, and E. Barrado, *Talanta*, **72**, 282 (2007).
27. H. M. Nassef, A.-E. Radi, and C. O'Sullivan, *Anal. Chim. Acta*, **583**, 182 (2007).
28. H. M. Nassef, A.-E. Radi, and C. K. O'Sullivan, *Electrochem. Commun.*, **8**, 1719 (2007).
29. M. Huang, Y. Shao, X. Sun, H. Chen, B. Liu, and S. Dong, *Langmuir*, **21**, 323 (2005).
30. K. Shi and K.-K. Shiu, *Anal. Chem.*, **74**, 879 (2002).
31. G. K. Kiema, M. Aktay, and M. T. McDermott, *J. Electroanal. Chem.*, **540**, 7 (2003).
32. K. K. Shiu and K. Shi, *Electroanalysis*, **10**, 959 (1998).
33. K. K. Shiu and F. Y. Song, *Electroanalysis*, **10**, 256 (1998).
34. K. K. Shiu and K. Shi, *Electroanalysis*, **12**, 134 (2000).
35. N. Vettorazzi, L. Otero, and L. Sereno, *J. Electrochem. Soc.*, **148**, E413 (2001).
36. S. Yamazaki, Z. Siroma, T. Ioroi, K. Tanimoto, and K. Yasuda, *Carbon*, **45**, 256 (2007).
37. G. Liu, J. Liu, T. Böcking, P. K. Eggers, and J. J. Gooding, *Chem. Phys.*, **319**, 136 (2007).
38. A. C. Cruickshank, E. S. Q. Tan, P. A. Brooksby, and A. J. Downard, *Electrochem. Commun.*, **9**, 1456 (2007).
39. C. A. McDermott, K. R. Kneten, and R. L. McCreery, *J. Electrochem. Soc.*, **140**, 2593 (1993).
40. R. Kötz, D. Alliata, C. Barbero, M. Bärtsch, A. Braun, R. Imhof, B. Schnyder, and M. Sullivan, Paper 85, *193rd Meeting of The Electrochemical Society*, San Diego, CA, May 3–8, 1998.
41. C. Barbero, J. J. Silber, and L. Sereno, *J. Electroanal. Chem. Interfacial Electrochem.*, **248**, 321 (1988).
42. R. A. Osteryoung, G. Lauer, and F. Anson, *Anal. Chem.*, **34**, 1833 (1962).
43. P. Chen, M. A. Fryling, and R. L. McCreery, *Anal. Chem.*, **67**, 3115 (1999).
44. G. Ilangovan and K. Chandrasekara Pillai, *J. Solid State Electrochem.*, **3**, 357 (1999).
45. L. J. Kepley and A. J. Bard, *Anal. Chem.*, **60**, 1459 (1988).
46. K. K. Cline, M. T. McDermott, and R. L. McCreery, *J. Phys. Chem.*, **98**, 5314 (1994).
47. M. G. Sullivan, R. Kötz, and O. Haas, *J. Electrochem. Soc.*, **147**, 308 (2000).